

Short communication

Synthesis and electrochemical properties of $\text{Li}_{1-x}\text{Fe}_{0.8}\text{Ni}_{0.2}\text{O}_2\text{-Li}_x\text{MnO}_2$ ($\text{Mn}/(\text{Fe} + \text{Ni} + \text{Mn}) = 0.8$) material

G.J. Park^a, Y.S. Lee^{a,*}, J. Kim^b, K.S. Nahm^c, Y. Sato^d

^a Faculty of Applied Chemical Engineering, Chonnam National University, 300 Yongbong-dong, Gwangju 500-757, Republic Korea

^b Department of Material Science and Engineering, Chonnam National University, 300 Yongbong-dong, Gwangju 500-757, Republic Korea

^c School of Chemical Engineering and Technology, Chonbuk National University, 664-14 Duckjin-dong, Chonju 561-756, Republic Korea

^d Department of Applied Chemistry, Kanagawa University, 3-27-1 Rokkakubashi, Kanagawa-ku, Yokohama 221-8686, Japan

Available online 28 June 2007

Abstract

A new type of $\text{Li}_{1-x}\text{Fe}_{0.8}\text{Ni}_{0.2}\text{O}_2\text{-Li}_x\text{MnO}_2$ ($\text{Mn}/(\text{Fe} + \text{Ni} + \text{Mn}) = 0.8$) material was synthesized at 350 °C in air atmosphere using a solid-state reaction. The material had an XRD pattern that closely resembled that of the original $\text{Li}_{1-x}\text{FeO}_2\text{-Li}_x\text{MnO}_2$ ($\text{Mn}/(\text{Fe} + \text{Mn}) = 0.8$) with much reduced impurity peaks. The $\text{Li}/\text{Li}_{1-x}\text{Fe}_{0.8}\text{Ni}_{0.2}\text{O}_2\text{-Li}_x\text{MnO}_2$ cell showed a high initial discharge capacity above 192 mAh g⁻¹, which was higher than that of the parent $\text{Li}/\text{Li}_{1-x}\text{FeO}_2\text{-Li}_x\text{MnO}_2$ (186 mAh g⁻¹). We expected that the increase of initial discharge capacity and the change of shape of discharge curve for the $\text{Li}/\text{Li}_{1-x}\text{Fe}_{0.8}\text{Ni}_{0.2}\text{O}_2\text{-Li}_x\text{MnO}_2$ cell is the result from the redox reaction from Ni²⁺ to Ni³⁺ during charge/discharge process. This cell exhibited not only a typical voltage plateau in the 2.8 V region, but also an excellent cycle retention rate (96%) up to 45 cycles.

© 2007 Elsevier B.V. All rights reserved.

Keywords: Lithium secondary battery; Cathode material; $\text{Li}_{1-x}\text{FeO}_2\text{-Li}_x\text{MnO}_2$; $\text{Li}_{1-x}\text{Fe}_{0.8}\text{Ni}_{0.2}\text{O}_2\text{-Li}_x\text{MnO}_2$

1. Introduction

The presently commercialized lithium secondary batteries use layer structured LiCoO_2 cathode material. LiCoO_2 has a rock salt structure where lithium and transition metal cation occupy alternate layers of octahedral sites in a distorted close-packed oxygen ion lattice. It will use a power source for small portable electronic devices for some time because it showed stable charge/discharge profile and an excellent cycleability, although it had a high cost and toxicity of cobalt [1–3].

Recently, it has become painfully evident that new cathode materials are required for large scale battery operations that meet the dual requirements of cost and safety, in order to successfully commercialize hybrid electric vehicle (HEV). The LiMn_2O_4 spinel is the most prospecting cathode material at present, but Fe-based material is also one of the strong candidates for large scale lithium secondary battery system [4–6]. However, it is also

well known that the $\text{Fe}^{4+/3+}$ redox energy in the LiFeO_2 structure tends to lie too far below the Fermi energy of the lithium anode and the $\text{Fe}^{3+}/\text{Fe}^{2+}$ couple is too close to it. This indication results in the low charge/discharge profile and strongly prevent the use of LiFeO_2 as a practical cathode material. In an attempt to solving this problem, Lee et al. developed a new type of the solid solution $\text{Li}_{1-x}\text{FeO}_2\text{-Li}_x\text{MnO}_2$ ($\text{Mn}/(\text{Fe} + \text{Mn}) = 0.1\text{--}0.5$) materials [7–16]. In particular, the Li/50% Mn-substituted LiFeO_2 system exhibited an excellent cyclic behavior for up to 50 cycles as well as a higher distinct voltage plateau (2.8 V) region against that of Li/LiFeO_2 [17].

In previous report [17], we also found that Li/50% Mn-substituted LiFeO_2 cell showed a small initial discharge capacity (137 mAh g⁻¹) and final discharge capacity (158 mAh g⁻¹) after a long-term cycling. The discharge capacity of above system was still unsatisfactory as a practical lithium secondary battery. However, we believe it was quite noteworthy from the viewpoint of cost and environmental aspect because this system consisted of two main cheap transition metals (Fe and Mn).

In this paper, we report a new type of $\text{Li}_{1-x}\text{Fe}_{0.8}\text{Ni}_{0.2}\text{O}_2\text{-Li}_x\text{MnO}_2$ ($\text{Mn}/(\text{Fe} + \text{Ni} + \text{Mn}) = 0.8$) material, which

* Corresponding author.

E-mail address: leeyes@chonnam.ac.kr (Y.S. Lee).

shows a high initial discharge capacity and an excellent cycle retention rate after a long-term cycling. We suggest that this trial can be a very important thing to develop a new cathode material with high energy density for large scale batteries.

2. Experimental

$\text{Li}_{1-x}\text{Fe}_{0.8}\text{Ni}_{0.2}\text{O}_2\text{-Li}_x\text{MnO}_2$ material ($\text{Mn}/(\text{Fe} + \text{Ni} + \text{Mn}) = 0.8$) was synthesized using $\text{LiOH}\cdot\text{H}_2\text{O}$ (Kishida Chemical, Japan), $\gamma\text{-FeOOH}$ (High Purity Chemicals, Japan), $\text{Ni}(\text{OH})_2$ (Wako Chemical, Japan), and $\gamma\text{-MnOOH}$ (Tosoh Chemical, Japan) using a solid-state method. A stoichiometric amount of each material was ground and calcined at 300°C for 10 h and 350°C for 10 h in air atmosphere using a box furnace. The thermal decomposition behavior of the precursors was examined by means of thermogravimetric analysis and different thermal analysis using a thermal analyzer system (TGA, DTA, Q600, TA Instruments, USA). A thin Pt plate was used as the sample holder. The powder was heated at 5°C min^{-1} and cooled at $10^\circ\text{C min}^{-1}$ in Ar flow. The Li, Fe, Ni and Mn contents in the resulting material were analyzed by atomic absorption spectroscopy (AAS, AA-6200, Shimadzu, Japan) after dissolving powdered in dilute nitric acid. The powder X-ray diffraction (XRD, Rint 1000, Rigaku, Japan) using $\text{CuK}\alpha$ radiation was used to identify the crystalline phase of the synthesized material. The particle morphologies of the resulting compound were observed using a scanning electron microscope (FE-SEM, S-4700, Hitachi, Japan). The electrochemical characterizations were performed using CR2032 coin-type cell. The cathode was fabricated with 20 mg of accurately weighed active material and 12 mg of conductive binder (8 mg of Teflonized acetylene black (TAB) and 4 mg of graphite). It was pressed on 200 mm^2 stainless steel mesh used as the current collector under a pressure of 300 kg cm^{-2} and dried at 130°C for 5 h in an oven. The test cell was made of a cathode and a lithium metal anode separated by a porous polypropylene film (Celgard 3401). The electrolyte used was a mixture of 1 M LiPF_6 -ethylene carbonate (EC)/dimethyl carbonate (DMC) (1:2 by vol., Ube Chemicals, Japan). The charge and discharge current density was 0.4 mA cm^{-2} with a cut-off voltage of 1.5–4.5 V at room temperature.

3. Results and discussion

The thermogravimetric and differential thermal analyses of the two precursors are shown in Fig. 1. The $\text{Li}_{1-x}\text{FeO}_2\text{-Li}_x\text{MnO}_2$ and $\text{Li}_{1-x}\text{Fe}_{0.8}\text{Ni}_{0.2}\text{O}_2\text{-Li}_x\text{MnO}_2$ in this study means $\text{Li}_{1-x}\text{FeO}_2\text{-Li}_x\text{MnO}_2$ ($\text{Mn}/(\text{Fe} + \text{Mn}) = 0.8$) and $\text{Li}_{1-x}\text{Fe}_{0.8}\text{Ni}_{0.2}\text{O}_2\text{-Li}_x\text{MnO}_2$ ($\text{Mn}/(\text{Fe} + \text{Ni} + \text{Mn}) = 0.8$), respectively, without any explanation. The precursor of $\text{Li}_{1-x}\text{FeO}_2\text{-Li}_x\text{MnO}_2$ material (LiOH , $\gamma\text{-FeOOH}$, and $\gamma\text{-MnOOH}$) as shown in Fig. 1(a) shows two distinct endothermic peaks on the DTA curve. The first distinct peak around 80°C is due to the removal of water from $\text{LiOH}\cdot\text{H}_2\text{O}$. The second peak at 260°C shows the formation of $\beta\text{-MnO}_2$. It is slightly moved at higher temperature against the 50% $\text{Li}_{1-x}\text{FeO}_2\text{-Li}_x\text{MnO}_2$ material in the previous report [17], which results from the

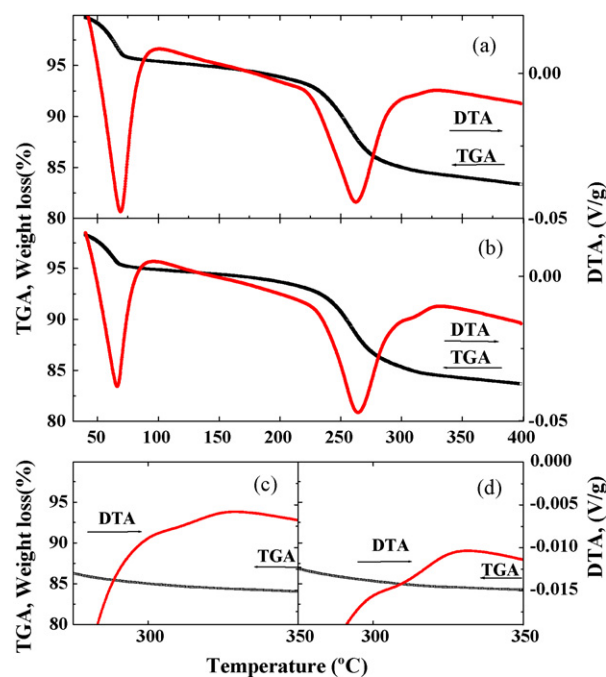


Fig. 1. Thermal analysis of (a) $\text{Li}_{1-x}\text{FeO}_2\text{-Li}_x\text{MnO}_2$ ($\text{Mn}/(\text{Fe} + \text{Mn}) = 0.8$) and (b) $\text{Li}_{1-x}\text{Fe}_{0.8}\text{Ni}_{0.2}\text{O}_2\text{-Li}_x\text{MnO}_2$ ($\text{Mn}/(\text{Fe} + \text{Ni} + \text{Mn}) = 0.8$).

larger Mn content (80%) in the precursor for this study. However, $\text{Li}_{1-x}\text{Fe}_{0.8}\text{Ni}_{0.2}\text{O}_2\text{-Li}_x\text{MnO}_2$ material, which consists with LiOH , $\gamma\text{-FeOOH}$, $\text{Ni}(\text{OH})_2$, and $\gamma\text{-MnOOH}$, shows one additional small DTA peak. It results from the decomposition of $\text{Ni}(\text{OH})_2$ to form a NiO and H_2O above 200°C . Although it shows a very trifle difference between two DTA curves, we could clearly find the gap of curve shape as shown in Fig. 1(c and d). Also, there are a couple of slight difference between original and nickel substituted $\text{Li}_{1-x}\text{FeO}_2\text{-Li}_x\text{MnO}_2$ material during the X-ray diffraction, cycle test, and electrochemical analyses. We expected the nickel ion in the $\text{Li}_{1-x}\text{Fe}_{0.8}\text{Ni}_{0.2}\text{O}_2\text{-Li}_x\text{MnO}_2$ material can important role to change the structural property of original $\text{Li}_{1-x}\text{FeO}_2\text{-Li}_x\text{MnO}_2$ material.

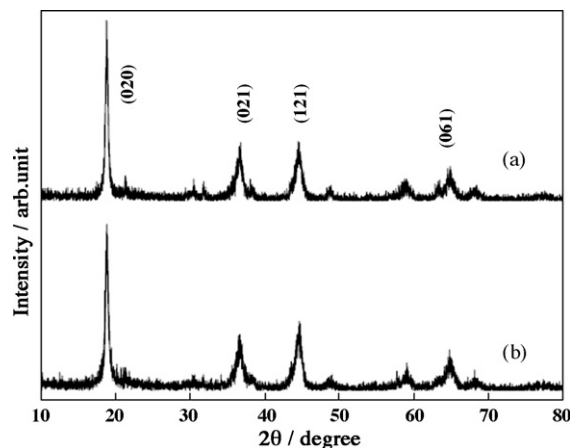


Fig. 2. XRD patterns of (a) $\text{Li}_{1-x}\text{FeO}_2\text{-Li}_x\text{MnO}_2$ ($\text{Mn}/(\text{Fe} + \text{Mn}) = 0.8$) and (b) $\text{Li}_{1-x}\text{Fe}_{0.8}\text{Ni}_{0.2}\text{O}_2\text{-Li}_x\text{MnO}_2$ ($\text{Mn}/(\text{Fe} + \text{Ni} + \text{Mn}) = 0.8$). These materials were calcined at 350°C for 10 h in air.

Fig. 2 shows X-ray diffraction (XRD) patterns of the original $\text{Li}_{1-x}\text{FeO}_2\text{-Li}_x\text{MnO}_2$ and the $\text{Li}_{1-x}\text{Fe}_{0.8}\text{Ni}_{0.2}\text{O}_2\text{-Li}_x\text{MnO}_2$, which were calcined at 350°C for 15 h in air atmosphere. In order to synthesize homogeneous materials, each starting material was thoroughly mixed and pressed at a 300 kg cm^{-2} pressure into a 20 mm diameter pellet to improve the activity between the particles of the precursor. As previously reported [17], Lee et al. expected that the Mn ion (ionic radius of Mn^{3+} is 0.72 \AA) could be easily substituted at the Fe(2a) site of orthorhombic LiFeO_2 material because it has a similar ionic radius compared to that of Fe^{3+} (0.69 \AA) ion. However, they concluded that $\text{LiFe}_{1-x}\text{Mn}_x\text{O}_2$ material is impossible to form a perfect solid solution directly. Because Mn ions can not substitute into LiFeO_2 structure at low synthetic temperature (150°C), but that as a result it forms a mixture of LiFeO_2 and MnO . This presents a strong barrier to the development of $\text{LiFe}_{1-x}\text{Mn}_x\text{O}_2$ material at low temperature, but can be a starting point to develop a new $\text{Li}_{1-x}\text{FeO}_2\text{-Li}_x\text{MnO}_2$ cathode material at higher synthetic temperature (350°C).

Be based on this result, it was conducted the substitution of nickel doping in a different way. In order to easily substitute nickel ions into the iron site in the $\text{Li}_{1-x}\text{FeO}_2\text{-Li}_x\text{MnO}_2$ material, we synthesized $\text{LiFe}_{0.8}\text{Ni}_{0.2}\text{O}_2$ mixture (only stoichiometric content) in advance and then added the Mn source before the calcination process at 350°C . We expected that the iron ions in $\text{Li}_{1-x}\text{FeO}_2\text{-Li}_x\text{MnO}_2$ could be replaced by nickel ions more easily against that of orthorhombic LiFeO_2 material, because $\text{Li}_{1-x}\text{FeO}_2\text{-Li}_x\text{MnO}_2$ system easily forms a solid solution at 350°C with various transition metals.

$\text{Li}_{1-x}\text{FeO}_2\text{-Li}_x\text{MnO}_2$ material in this study exhibited an XRD pattern resembling that of the orthorhombic Li_xMnO_2 (*Pnam*) material [18]. Some of main peaks, (020) and (021), of $\text{Li}_{1-x}\text{FeO}_2\text{-Li}_x\text{MnO}_2$ system increased as the Mn content increased.

$\text{Li}_{1-x}\text{Fe}_{0.8}\text{Ni}_{0.2}\text{O}_2\text{-Li}_x\text{MnO}_2$ presents a well-developed XRD pattern as compared with that of original $\text{Li}_{1-x}\text{FeO}_2\text{-Li}_x\text{MnO}_2$ material. This material showed slightly reduced impurity peaks between 25° and 35° region. Also, it was found that some additional impurity peaks at $2\theta = 37^\circ$ and $2\theta = 64^\circ$ of $\text{Li}_{1-x}\text{FeO}_2\text{-Li}_x\text{MnO}_2$ were clearly reduced from the XRD diagram. It means that doped nickel ions were successfully substituted and stabilized into the $\text{Li}_{1-x}\text{FeO}_2\text{-Li}_x\text{MnO}_2$ structure and enhanced the crystallographic characterization of original $\text{Li}_{1-x}\text{FeO}_2\text{-Li}_x\text{MnO}_2$ material.

Fig. 3 shows scanning electron microscopy (SEM) images of the $\text{Li}_{1-x}\text{FeO}_2\text{-Li}_x\text{MnO}_2$ and the $\text{Li}_{1-x}\text{Fe}_{0.8}\text{Ni}_{0.2}\text{O}_2\text{-Li}_x\text{MnO}_2$ materials. As reported in a previous study [17], 50% Mn-substituted LiFeO_2 material consisted with large particles at about 500–600 nm and other small particles at about 100–200 nm were distributed among the larger particles. Two materials in this study, these also show a similar particle size and a particle distribution. A small part of needle-like large particle were located randomly and lots of small particle at about 100 nm were distributed among the larger particles. In the case of $\text{Li}_{1-x}\text{Fe}_{0.8}\text{Ni}_{0.2}\text{O}_2\text{-Li}_x\text{MnO}_2$, it shows slightly diminished particle size and more rounded shape compare with that of original $\text{Li}_{1-x}\text{FeO}_2\text{-Li}_x\text{MnO}_2$ material.

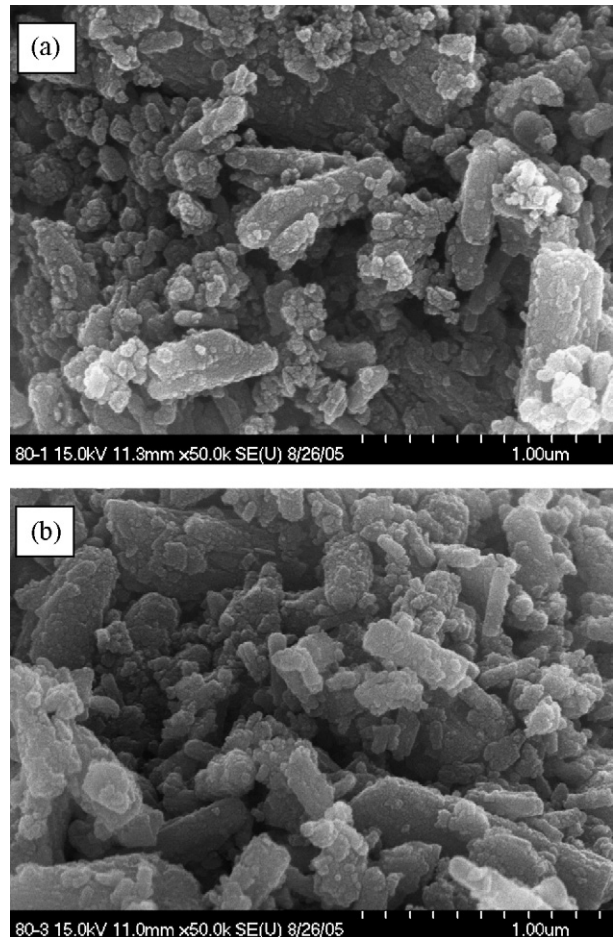


Fig. 3. SEM images of (a) $\text{Li}_{1-x}\text{FeO}_2\text{-Li}_x\text{MnO}_2$ ($\text{Mn}/(\text{Fe} + \text{Mn}) = 0.8$) and (b) $\text{Li}_{1-x}\text{Fe}_{0.8}\text{Ni}_{0.2}\text{O}_2\text{-Li}_x\text{MnO}_2$ ($\text{Mn}/(\text{Fe} + \text{Ni} + \text{Mn}) = 0.8$) materials.

Fig. 4 shows the electrochemical characterizations of the $\text{Li}/\text{Li}_{1-x}\text{FeO}_2\text{-Li}_x\text{MnO}_2$ and the $\text{Li}/\text{Li}_{1-x}\text{Fe}_{0.8}\text{Ni}_{0.2}\text{O}_2\text{-Li}_x\text{MnO}_2$ systems. The test condition was a current density of 0.4 mA cm^{-2} between 4.5 and 1.5 V. The first

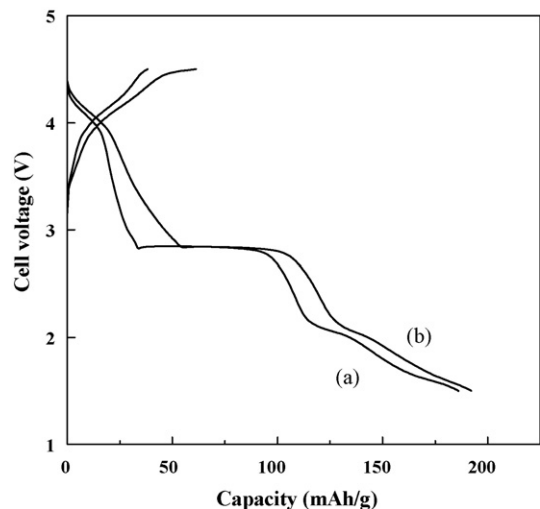


Fig. 4. Charge/discharge curves and specific discharge capacity of (a) $\text{Li}/\text{Li}_{1-x}\text{FeO}_2\text{-Li}_x\text{MnO}_2$ ($\text{Mn}/(\text{Fe} + \text{Mn}) = 0.8$) and (b) $\text{Li}/\text{Li}_{1-x}\text{Fe}_{0.8}\text{Ni}_{0.2}\text{O}_2\text{-Li}_x\text{MnO}_2$ ($\text{Mn}/(\text{Fe} + \text{Ni} + \text{Mn}) = 0.8$) cells.

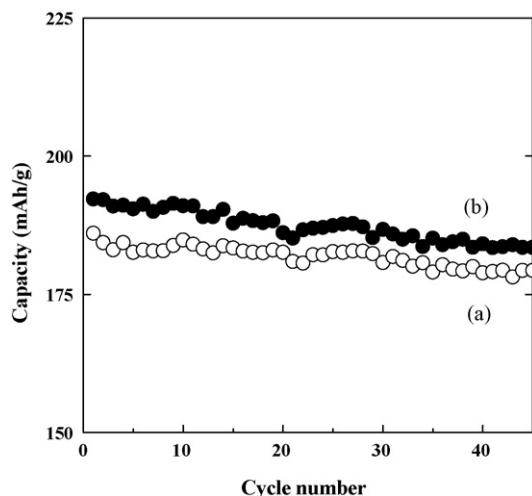


Fig. 5. Specific discharge capacity vs. cycle number for the (a) $\text{Li/Li}_{1-x}\text{FeO}_2\text{-Li}_x\text{MnO}_2$ ($\text{Mn}/(\text{Fe} + \text{Mn}) = 0.8$) and (b) $\text{Li/Li}_{1-x}\text{Fe}_{0.8}\text{Ni}_{0.2}\text{O}_2\text{-Li}_x\text{MnO}_2$ ($\text{Mn}/(\text{Fe} + \text{Ni} + \text{Mn}) = 0.8$) cells.

charge/discharge curve of the $\text{Li/Li}_{1-x}\text{FeO}_2\text{-Li}_x\text{MnO}_2$ cell is shown in Fig. 4(a). It shows a high initial discharge capacity over 186 mAh g^{-1} and also a distinct voltage plateaus at 2.8 V in the discharge curve. The capacity difference (49 mAh g^{-1}) between 50 and 80% $\text{Li}_{1-x}\text{FeO}_2\text{-Li}_x\text{MnO}_2$ systems appears to be the result in amount of substituting Mn ions in this system [17]. Fig. 4(b) presents the initial discharge behavior of $\text{Li/Li}_{1-x}\text{Fe}_{0.8}\text{Ni}_{0.2}\text{O}_2\text{-Li}_x\text{MnO}_2$ cell. It was interesting to find a difference in discharge capacities between 2.8 and 4.5 V (herein referred to as $C_{2.8-4.5 \text{ V}}$) of the two systems, although the two cells showed very similar cycle behavior. The $C_{2.8-4.5 \text{ V}}$ values were 37 and 57 mAh g^{-1} for the $\text{Li/Li}_{1-x}\text{FeO}_2\text{-Li}_x\text{MnO}_2$ cell and the $\text{Li/Li}_{1-x}\text{Fe}_{0.8}\text{Ni}_{0.2}\text{O}_2\text{-Li}_x\text{MnO}_2$ cell, respectively. The difference of $C_{2.8-4.5 \text{ V}}$ between the two cells was quite a large and up to 20 mAh g^{-1} , which was a considerable total discharge capacity. The $\text{Li/Li}_{1-x}\text{Fe}_{0.8}\text{Ni}_{0.2}\text{O}_2\text{-Li}_x\text{MnO}_2$ cell exhibited a high initial discharge capacity of 192 mAh g^{-1} , even though all increased capacity of $C_{2.8-4.5 \text{ V}}$ did not reflected.

One interesting thing, this indication is conflicted with LiMeO_2 systems ($\text{Me} = \text{Co}, \text{Ni}, \text{Mn}, \text{etc.}$) [19–21], which generally showed a reduced discharge capacity by doped other transition metals in the Me(3a) site. Conversely, it means that nickel ions might be played an effective role in increasing the initial discharge capacity of the $\text{Li}_{1-x}\text{Fe}_{0.8}\text{Ni}_{0.2}\text{O}_2\text{-Li}_x\text{MnO}_2$ material during synthesis and electrochemical processes. We also found that the valence state of Fe, Ni, and Mn ions in the 80% $\text{Li}_{1-x}\text{Fe}_{0.8}\text{Ni}_{0.2}\text{O}_2\text{-Li}_x\text{MnO}_2$ material are +3, +2, and +4, respectively, using XPS analysis. We suggest that the increase of initial discharge capacity and the change of shape of discharge curve for the $\text{Li/Li}_{1-x}\text{Fe}_{0.8}\text{Ni}_{0.2}\text{O}_2\text{-Li}_x\text{MnO}_2$ cell is the result from the redox reaction from Ni^{2+} to Ni^{3+} during charge/discharge process. A more detailed discussion about role and effect of doped nickel ion in the $\text{Li}_{1-x}\text{Fe}_{0.8}\text{Ni}_{0.2}\text{O}_2\text{-Li}_x\text{MnO}_2$ material using EXAFS, and XPS will be reported elsewhere.

Fig. 5 shows the variation in the specific discharge capacity with the number of cycles for the above two systems. As reported

before [17], $\text{Li}/50\% \text{Li}_{1-x}\text{FeO}_2\text{-Li}_x\text{MnO}_2$ cell exhibited a small initial discharge capacity of 137 mAh g^{-1} and slightly increased capacity (158 mAh g^{-1}) until 50th cycle. It should be noted that this discharge capacity still falls short of that required for a practical battery system with high discharge capacity. The $\text{Li}/\text{Li}_{1-x}\text{FeO}_2\text{-Li}_x\text{MnO}_2$ cell presented a high discharge capacity of 186 mAh g^{-1} and this cell continuously decreased during cycling. However, $\text{Li}/\text{Li}_{1-x}\text{Fe}_{0.8}\text{Ni}_{0.2}\text{O}_2\text{-Li}_x\text{MnO}_2$ cell showed a very high initial discharge capacity of 192 mAh g^{-1} and also an excellent cycle retention rate of 96% after 45th cycle. Although the difference of capacities between two cells is not so big, this increased discharge capacity of $\text{Li}/\text{Li}_{1-x}\text{Fe}_{0.8}\text{Ni}_{0.2}\text{O}_2\text{-Li}_x\text{MnO}_2$ cell is reproducible and maintained as its initial behavior during cycling test.

4. Conclusion

A new type of $\text{Li}_{1-x}\text{Fe}_{0.8}\text{Ni}_{0.2}\text{O}_2\text{-Li}_x\text{MnO}_2$ ($\text{Mn}/(\text{Fe} + \text{Ni} + \text{Mn}) = 0.8$) material was synthesized at $350 \text{ }^\circ\text{C}$ in air atmosphere using a solid-state reaction. The material had an XRD pattern that closely resembled that of the original $\text{Li}_{1-x}\text{FeO}_2\text{-Li}_x\text{MnO}_2$ ($\text{Mn}/(\text{Fe} + \text{Mn}) = 0.8$) with much reduced impurity peaks. The $\text{Li}/\text{Li}_{1-x}\text{Fe}_{0.8}\text{Ni}_{0.2}\text{O}_2\text{-Li}_x\text{MnO}_2$ cell showed a high initial discharge capacity above 192 mAh g^{-1} , which was higher than that of the parent $\text{Li}/\text{Li}_{1-x}\text{FeO}_2\text{-Li}_x\text{MnO}_2$ (186 mAh g^{-1}). This cell exhibited not only a typical voltage plateau in the 2.8 V region, but also an excellent cycle retention rate (96%) up to 45 cycles. We expected that increased discharge capacity resulted from the redox reaction of nickel ions during charge/discharge process. We believe that 80% $\text{Li}_{1-x}\text{Fe}_{0.8}\text{Ni}_{0.2}\text{O}_2\text{-Li}_x\text{MnO}_2$ could be a new type of cathode material by optimizing the substituted Ni content.

Acknowledgement

This work was supported by Korea Electrical Engineering & Science Research Institute by Korea Government (2006).

References

- [1] K. Mizushima, P.C. Jones, P.J. Wiseman, J.B. Goodenough, *Mater. Res. Bull.* 15 (1980) 783.
- [2] E. Rossen, J.N. Reimers, J.R. Dahn, *Solid State Ionics* 62 (1993) 53.
- [3] T. Ohzuku, A. Ueda, M. Nagayama, Y. Iwakoshi, H. Komori, *Electrochimica Acta* 38 (1993) 1159.
- [4] D.H. Jang, Y.J. Shin, S.M.H. Oh, *J. Electrochem. Soc.* 143 (1996) 2204.
- [5] Y. Xia, Y. Zhou, M. Yoshio, *J. Electrochem. Soc.* 144 (1997) 2593.
- [6] Y.S. Lee, C.S. Yoon, Y.K. Sun, M. Yoshio, *Electrochem. Solid-State Lett.* 5 (1) (2002) A1.
- [7] R. Kanno, T. Shirane, Y. Kawamoto, Y. Takeda, M. Takano, M. Ohashi, Y. Yamaguchi, *J. Electrochem. Soc.* 146 (1996) 2435.
- [8] T. Shirane, R. Kanno, Y. Kawamoto, Y. Takeda, M. Takano, T. Kamiyama, F. Izumi, *Solid State Ionics* 79 (1995) 227.
- [9] M. Tabuchi, K. Ado, H. Sakaebe, C. Masquelier, H. Kageyama, O. Nakamura, *Solid State Ionics* 79 (1995) 220.
- [10] M. Tabuchi, C. Masquelier, T. Takeuchi, K. Ado, I. Matsubara, T. Shirane, R. Kanno, S. Tsutsui, S. Nasu, H. Sakaebe, O. Nakamura, *Solid State Ionics* 90 (1996) 129.
- [11] K. Ado, M. Tabuchi, H. Kobayashi, H. Kageyama, O. Nakamura, Y. Inaba, R. Kanno, M. Takagi, Y. Takeda, *J. Electrochem. Soc.* 144 (1997) L177.

- [12] M. Tabuchi, S. Tsutsui, C. Masquelier, R. Kanno, K. Ado, I. Matsubara, S. Nasu, H. Kageyama, *J. Solid State Chem.* 140 (1998) 159.
- [13] M. Tabuchi, K. Ado, H. Kobayashi, I. Matsubara, H. Kageyama, M. Wakita, S. Tsutsui, S. Nasu, Y. Takeda, C. Masquelier, A. Hirano, R. Kanno, *J. Solid State Chem.* 141 (1998) 554.
- [14] Y. Sakurai, H. Arai, S. Okada, J. Yamaki, *J. Power Sources* 68 (1997) 711.
- [15] Y. Sakurai, H. Arai, J. Yamaki, *Solid State Ionics* 113–115 (1998) 29.
- [16] Y.S. Lee, C.S. Yoon, Y.K. Sun, K. Kobayakawa, Y. Sato, *Electrochem. Comm.* 4 (2002) 727.
- [17] Y.S. Lee, S. Sato, Y.K. Sun, K. Kobayakawa, Y. Sato, *Electrochem. Comm.* 5 (2002) 359.
- [18] Y. Xia, M. Yoshio, *J. Power Sources* 57 (1995) 125.
- [19] C. Delmas, I. Saadoune, A. Rougier, *J. Power Sources* 44 (1993) 595.
- [20] Y.I. Jang, B. Huang, H. Wang, D.R. Sadoway, Y.M. Chiang, *J. Electrochem. Soc.* 146 (1999) 3217.
- [21] J. Kim, K. Amine, *J. Power Sources* 104 (2002) 33.